

Serpentinization as a route to liberating phosphorus on habitable worlds

Matthew Pasek (✉ mpasek@usf.edu)

School of Geosciences, University of South Florida <https://orcid.org/0000-0003-1280-9555>

Arthur Omran

School of Geosciences, University of South Florida

Carolyn Lang

School of Geosciences, University of South Florida

Maheen Gull

School of Geosciences, University of South Florida

Josh Abbatiello

School of Geosciences, University of South Florida

Tian Feng

School of Geosciences, University of South Florida

Lyle Garong

School of Geosciences, University of South Florida

Heather Abbott-Lyon

Department of Chemistry, Kennesaw State University

Article

Keywords: Habitability, Serpentinization, Redox, Phosphorus

Posted Date: July 9th, 2020

DOI: <https://doi.org/10.21203/rs.3.rs-37651/v1>

License:  This work is licensed under a Creative Commons Attribution 4.0 International License.

[Read Full License](#)

Abstract

Planetary habitability is in part governed by nutrient availability, including the availability of the element phosphorus. The nutrient phosphorus plays roles in various necessary biochemical functions, and its biogeochemical cycling has been proposed to be extremely slow due to a strong coupling to the rock cycle via mineral weathering. Here we show a route to P liberation from water-rock reactions that are thought to be common throughout the Solar System. We report the speciation of phosphorus in serpentinite rocks to include the ion phosphite (HPO_3^{2-} with P^{3+}) and show that reduction of phosphate to phosphite is predicted from thermodynamic models of serpentinization. As a result, as olivine in ultramafic rocks alters to serpentine minerals, phosphorus as soluble phosphite should be released under low redox conditions, liberating this key nutrient for life. Thus, this element may be accessible to developing life where water is in direct contact with ultramafic rock, providing a source of this nutrient to potentially habitable worlds.

Introduction

Nutrients such as nitrogen (N) and phosphorus (P) limit ecosystem size in the absence of the evolutionary means to extract and/or fixate these elements. More specifically, the evolution of N fixation has generally resulted in P serving as the limiting nutrient in biomass [1]. Beyond the earth, planetary habitability is governed in part by nutrient availability, in addition to physical (pressure and temperature) and environmental (disequilibria) constraints. Phosphorus plays a critical role in biochemical functions [2–4], ranging from nucleic acids to metabolism, and as such, P is actively scavenged and recycled by ecosystems [1, 5], and presumably is important elsewhere for the development of life, though there may be routes to life without phosphorus [6, 7].

Phosphorus is unique amongst the major biogenic elements in that its elemental cycle excludes a significant volatile phase (although volatile phosphine is present as a minor constituent, as reported by [8, 9]). All phosphorus ultimately originates from rocks and minerals. Within felsic rocks rich in SiO_2 , most phosphate is associated with calcium phosphate minerals such as apatite ($\text{Ca}_5(\text{PO}_4)_3(\text{OH},\text{F},\text{Cl})$) or rare earth element (REE) phosphates such as monazite $(\text{REE})\text{PO}_4$. Within ultramafic, SiO_2 -poor rocks P instead is generally associated with olivine dissolving at up to 100 ppm within the crystal lattice, likely exchanging for Si in SiO_4 tetrahedra [10–15].

This dichotomy of P-bearing minerals in vastly different silicate rocks raises an important question for planetary habitability, including that of the early earth: which mineral source of phosphorus is more important in a given environment? For instance, the felsic rocks generally have more P, and this P is associated with apatite, which may dissolve via reactions with carbonate [16] or NH_4^+ and sulfate [17, 18] prior to biological extraction. In contrast, if ultramafic rocks are more abundant (as suggested by the dominance of olivine in the upper mantle [19, 20]), then the issue of a lower P abundance in olivine is overcome by the sheer volume of this mineral. In both scenarios, the liberation of phosphorus requires

water interacting with rock; in the case of felsic rocks this is through dissolution or ionic exchange with phosphate minerals, and in ultramafic rocks could occur through weathering and alteration of the rock.

The mode of availability of phosphorus as a nutrient would thus be dependent on the types of rock interacting with water in an environment. In the case of the early earth, ultramafic rocks are believed to have been more common due to the higher heat flux of upper mantle, which results in less differentiation and more ultramafic volcanism [21], the expression of which are the Archean komatiites [22]. Despite this likely dominance by ultramafic rocks, the Archean and Hadean both likely had some amount of more felsic rocks that comprised the early continents [23]. Beyond the earth the presumed habitable worlds include Mars, which bears a moderately SiO₂-rich crust with phosphate availability likely constrained by dissolution [24]. Phosphorus on the potentially habitable moons Europa and Enceladus is instead likely constrained by reactions of the subsurface oceans with ultramafic rock formed during accretion and differentiation [24–26]. Most P nutrient availability studies focus on felsic rock interactions such as dissolution [16–18, 24], and here we have chosen to investigate the potential for P liberation from more ultramafic sources, given their volumetric abundance for both the early earth and for icy ocean moons.

In addition to these intrinsic sources of phosphorus, extrinsic sources such as meteorites may have delivered P to the early earth, primarily as metal phosphides [28–33]. The advantage of such a source is that the reaction of water with phosphides liberates P as the ion phosphite (HPO₃²⁻) in which the oxidation state of P is +3 as opposed to +5. Phosphite salts are generally much more soluble than the comparable phosphate salts [34], and hence the presence of phosphite may be a plausible free source of P on a habitable world. However, such a source is less plausible for icy moons given the general difficulty of surface to ocean material transfer, as well as the fact that phosphides tend to be high-temperature, inner solar system phases [35].

Phosphite could be a P nutrient that would be more relevant to planetary habitability due to its higher solubility if there exist intrinsic sources. However, a dominant paradigm of phosphorus geochemistry is that phosphorus is synonymous with phosphate. This assumption is generally driven by the fact that the first redox transition—from phosphate to phosphite—occurs at conditions more reducing than the water-H₂ reduction potential (-0.35 V for phosphate reduction vs. 0 V at pH 0 for water to H₂). A second assumption is that the oxidation of reduced forms of P such as phosphite proceeds rapidly so that even if phosphite is formed, it will oxidize to phosphate quickly enough that phosphate's chemical behavior effectively describes the bulk geochemistry of phosphorus on the earth's surface. Although the latter assumption has been shown untrue [31, 34] based on oxidation rate experiments of phosphite as salts and in solution [36], the former still presents a conundrum: can reduced oxidation state P be generated in water-rich environments?

Such a question is especially pertinent to planetary habitability, including the habitability of the early earth. The poor solubility of phosphate could limit the availability of P on those planets where plate tectonic activity is minimal [37], as the cycling of rock would not renew P sources. Alternatively, planets dominated by ultramafic rocks may not have abundant apatite as a source of P from weathering, given

the generally low abundance of P in ultramafic rocks [38]. Considering the importance of P in modern biochemical functions from nucleic acids to metabolic pathways [2], this low solubility or abundance could negatively impact the fecundity of a potentially habitable planet. However, if P is reduced from phosphate to phosphite, then the solubility of P is no longer constrained by poorly soluble phosphate minerals.

For this reason, if there were a route to transforming phosphate to phosphite in a widespread fashion, then the precipitation of phosphate would not deplete total P concentrations, allowing P to persist in the aqueous environment as an accessible nutrient. Recently, iron oxidation has been shown to correspond to a concomitant reduction of phosphate to phosphite in iron-rich sediments [34]. Additionally, a role for P redox in biochemistry has been recognized [39], suggesting there might exist a source of reduced P in the environment [40]. We explore here the possibility that electrochemically reducing water-rock interactions—namely the hydration and oxidation of olivine—result in the production of phosphite, in a way more general than the coupling of Fe^{2+} to phosphate reduction or through other sources [41]. Given the prevalence of mafic and ultramafic rock in the outer solar system [42], liberation of P as phosphite from reaction of water with ultramafic minerals—even though such rocks are typically very low in total P (~100 ppm or less, [38])—may ultimately have been a highly plausible source of P due to the sheer volume of material available to react.

The interactions of water and rock lead to several mineralogical and solutional changes [43]. Rock can act as a buffer to water, moderating its pH by dissolution and exchange of H^+ with alkali elements. Rock can also be the cause of significant pH changes, due to the oxidation of minerals, such as sulfide oxidation leading to low pH, and brucite ($\text{Mg}(\text{OH})_2$) formation increasing pH. Furthermore, the redox conditions resulting from water-rock reactions includes production of reducing agents such as H_2 . The rock itself undergoes several changes, including formation of new minerals via hydration, ionic exchange, and dissolution/precipitation; many of these processes result in physical changes to the rock including fracturing induced by volumetric expansion.

The reaction of mafic and ultramafic rocks with water are well known to produce new minerals, predominantly clays, phyllosilicates, and oxides, typically on the timescales of years [44, 45]. Clays are the major product of basaltic water-rock reactions whereas oxides and phyllosilicates (primarily serpentine minerals) dominate ultramafic water-rock reactions [46]. The latter process is known as serpentinization and forms serpentinite rocks, and is believed to be widespread in the solar system [47–49]). This process also is known to induce an environment that is both alkaline and reducing [50], and has been proposed as a location for the origin of life [51].

Results

Modeling of Water-Rock Reactions

Because the redox characteristics of the element phosphorus are typically limited to phosphate and its acid-base chemistry under “typical” aqueous conditions (Figure 1), the effect of water-rock interactions on P are viewed mostly in the context of dissolution of phosphate [52, 53]. However, it stands to reason that highly exergonic water-rock interactions could potentially promote the more intractable redox transition to phosphite. Alternatively, the speciation of phosphorus within such rocks may begin at a lower redox state than is typically considered (as phosphite exchanging with SiO₄ tetrahedra), as the speciation of P within olivine is unclear (and generally not considered as anything beyond +5 [10, 54]). As an example, the serpentinization of olivine couples the transformation of forsterite (Mg₂SiO₄) to serpentine minerals (Mg₃Si₂O₅(OH)₄), and the oxidation of fayalite (Fe₂SiO₄) to magnetite (Fe₃O₄), with the resulting mineralogy dependent on the initial stoichiometry of the olivine.



Brucite is formed when the Mg/Fe is greater than 3, and SiO₂ (typically amorphous) is formed when this ratio is less than 3. The oxidation of iron provides the electrons necessary to reduce neighboring material, whereas the serpentine mineral formation is exothermic, and provides the energy for the batch reaction [55-56]. We investigate the effect of serpentinization on P speciation by two methods: a redox calculation and by batch equilibrium models. First, we constrain the redox-pH conditions of the serpentinization reaction to show that these conditions are conducive to phosphate reduction. Thermodynamic construction of the Eh-pH diagram [57] are at a temperature of 298 K (25°C). The reaction of olivine (a solid solution mixture of Mg₂SiO₄ and Fe₂SiO₄) with water to give serpentine, magnetite, and hydrogen (H₂ to H⁺ + e⁻ as the half-cell), with SiO₂ as quartz or Mg(OH)₂ as brucite filling the stoichiometric balance from this reaction.

Notably, this result demonstrates that olivine serpentinization is conducive to phosphite production if the olivine is 50% forsterite or greater; however, reduction of a few percent of phosphate to phosphite still occurs at higher fayalite content (Figure 1). In general, most olivine is Mg-rich, favoring lower redox conditions.

As noted by Klein et al. [56] the serpentinization of mafic and ultramafic rocks generates H₂ only with the oxidation of Fe(II)-bearing minerals, and some of these minerals form solid solutions with serpentinization products, as ferrobucite, Fe(OH)₂, does with brucite, and greenalite, Fe₃Si₂O₅(OH)₄, does with Mg-serpentine minerals. To this end, olivine serpentinization was modeled using HSC Chemistry for batch equilibria at higher temperature and with more consideration for solid solutions, along with changing water/rock ratios, coupled to an investigation of P speciation. These models employed the equilibrium chemistry calculator as part of HSC Chemistry (version 7.1, Outokompu Research Oy)[1]. In these models, either the water to rock ratio was set to 1:1 (by mass) and temperature slowly increased, or the temperature was set to 250°C and the water to rock ratio increased (from ~0 to 0.25). The rock composition was set to be initially equivalent to 70% forsterite and 30% fayalite. We specifically modeled a dunite rock, where olivine is the sole silicate present, though similar test models with pyroxene present

did not substantially change the results with respect to phosphorus. The water reacting with the rock was set to a pH of 7.5, with 0.5 M NaCl, and low redox state (in equilibrium with an N₂ atmosphere). The system was held at a constant 500 bar pressure (50 MPa). We added data for ferrobrucite, greenalite, and minnesotaite [58], and the remainder of the data came from the existing HSC database. Solid solutions were assumed between olivine, serpentine minerals, talc minerals, and brucite. Due to a lack of thermodynamic data for reduced P compounds, and for P dissolved in olivine/glass, phosphorus was considered to be present in the rock as P₂O₅ at 1000 ppm of the total rock weight. Aqueous speciation was constrained using the Debye-Huckel approximation of activity coefficients. The pH was “fixed” with a buffer consisting of Na₂S/H₂S in a 1:4 ratio (0.1 M total Na added) that kept pH near 7.5. The species investigated in this model are provided in the methods below.

These batch equilibria models of an olivine dunite undergoing serpentinization reactions reveal that reduction of phosphate occurs readily at incipient serpentinization (i.e., at low water-rock ratios) (Figure 2). This is because water is potentially an oxidant for phosphite, and based on thermodynamic equilibria will ultimately oxidize phosphite to phosphate (though in practice it does not readily oxidize in water on timescales of greater than 5 years [34]). Reduced oxidation state P persists at about 0.3% of the total P even after the incipient serpentinization has completed (Figure 2b). These models, based off prior serpentinization batch equilibria models [58], demonstrate that reducing conditions pervade ultramafic rocks when the first interactions with water occur [59].

Phosphorus Reactions and Speciation

The above models demonstrate that the reduction of phosphate to phosphite is plausible within serpentinizing rock. This reduction occurs with the concomitant oxidation of iron, and is similar to prior work demonstrating iron oxidation coupled to phosphate reduction [34]. However, in contrast to the low production (1-4%) of phosphite reported by Fe²⁺ → Fe³⁺, these thermodynamic models predict the highly exergonic nature of serpentinization may be able to better power this reduction reaction than the amount produced by this diagenetic process, especially at low water to rock ratios.

We contrast these model results to P speciation within serpentinites. Serpentinites were collected from outcrops in southwestern Oregon at the Nolan Claim (N 42°10.003' W 123°42.709' and N 42°09.925' W 123°42.719') in Josephine County, OR, USA. These rocks are part of the Josephine Ophiolite in the Klamath Mountains [60, 61], and were a sequence of ultramafic rocks (dunite and harzburgite) with a formation age of 157 million years. Fresh samples were taken along the Josephine creek, then powdered and analyzed by Raman, XRD, and XRF. Both Raman and XRD show that the main mineralogy of these samples is the serpentine mineral antigorite (see SI). The composition of these rocks determined by XRF (see SI) shows they are composed primarily of magnetite and serpentine minerals, and that they are depleted in P and enriched in Cr and Ni (consistent with their ultramafic origin).

Phosphorus compounds were extracted from these serpentinites (see methods) and analyzed by ³¹P NMR spectroscopy (Figure 3). This spectrum shows a peak occurring within the region of phosphite that

splits (doublet at 4.9 and 1.4 ppm) when the coupling to hydrogen is permitted with a J_{P-H} coupling constant of 565 Hz. This coupling constant is diagnostic of phosphite [29], indicating phosphite is present within the serpentinite and is the major P species, formed during the highly reducing alteration of olivine. The other associated peaks correspond to phosphate (5.6 ppm) and pyrophosphate (-4.6 ppm). The presence of both phosphate and pyrophosphate may be due to a few causes. For one, the presence of phosphate may suggest incomplete reduction of phosphate to phosphite. Then, when the rock is serpentinitizing, the exergonic/exothermic reaction results in the dimerization of phosphate. Alternatively, and perhaps more likely, the presence of pyrophosphate and phosphate may suggest that phosphite has been oxidized by free radicals such as OH [62], possibly formed by reaction of O_2 with native metals present in the serpentinite [63], which may produce H_2O_2 that could then react to produce OH [64].

Modeling results and analysis of natural samples both demonstrate that P in ultramafic rocks that serpentinize is present in reduced form as phosphite. These results highlight a new role for serpentinitization in planetary habitability. In addition to heat generation and low redox conditions [65], serpentinitization also affects P speciation. Due to the higher solubility of phosphite relative to phosphate [66, 67], the serpentinitization process may liberate P into water as rocks serpentinize. Notably, the serpentinitized rock is significantly lower in total P content than associated unaltered rocks ([68, 69], Table S1). This may imply that as water reacts with the serpentinite that further extraction occurs due to the higher solubility of phosphite. As an illustration of this process, the addition of divalent cations (in this case, Ca^{2+}) to a solution of both phosphate and phosphite results in the precipitation of phosphate but leaves phosphite relatively unaffected (Figure 4). This implies that the phosphite is more soluble, and more easily extracted from the serpentinitizing rock than is phosphate.

Discussion

Nutrient availability is a key factor in what makes a world habitable. If P is an important constituent of biochemical processes beyond the earth, then understanding its liberation from rock provides constraints on habitability. We propose here that P in ultramafic rocks is liberated first by the transformation of phosphate to phosphite (or phosphite is intrinsic to olivine) through a coupled oxidation with iron, then the flushing of phosphite from the rock as water continues to react with it. To this end, this otherwise intractable element may become bioavailable for incipient life developing on other worlds, such as icy moons [27, 65], or on a primitive, ultramafic earth.

The results presented here are specific to serpentinitizing rock (and specifically, to three samples of serpentinite separated by a few tens of meters), which is necessarily ultramafic. Moreover, it is also not known if this process is common to serpentinites as only one rock outcrop was investigated (though these serpentinites are not especially unique). Mafic rocks, such as basalts, may not experience similar changes to P speciation [46], as serpentinitization is halted in these rocks by the production of ferrous clays, preventing the development of a redox driver for phosphate reduction. However, if oxidation of iron occurs as basalts alter under reduced conditions, then it may still be feasible that phosphate is reduced to

phosphite. As of yet, phosphite has not been reported as a species in basalt, through few analyses have been performed with proton coupling that could reveal P-H interactions [70–72].

Furthermore, these results do clearly show that phosphorus and phosphate are not synonymous in geologic systems, and great care should be taken in assuming that measured phosphorus (for instance, by ICP) is in fact phosphate and not the more soluble phosphite ion. The general assumption of P as phosphate needs closer inspection for those systems where redox may have occurred, especially the iron(II) to (III) transition, under otherwise anaerobic conditions.

The speciation of phosphorus within olivine is typically considered to be phosphate, with a substitution for a SiO_4 tetrahedron coupled to a vacancy or substitution by an alkali metal for the divalent metal position (to balance charge). The redox conditions of iron in olivine may be such that phosphorus is present instead in reduced form (for instance, $\text{Fe}^{2+} + \text{Si}^{4+}$ are substituted instead by Fe^{3+} and P^{3+}). Some olivine measurements have shown increases in Al^{3+} and Cr^{3+} with increasing P [10]. If such a conjecture is shown plausible, then P in olivine may intrinsically be present as phosphite in some cases.

Given that olivine is the dominant mineral of the upper mantle, and that the upper mantle makes up about 10% of the earth's total mass, P in olivine should have been a volumetrically significant source for the early earth, prior to the development of abundant crust. Additionally, the rocky material at the water-rock interface of several icy moons is likely composed of ultramafic rock. As such, the proposed redox reaction that then allows for the liberation of phosphorus may have been widely important for potentially habitable worlds. The liberation of this phosphite may have provided an abundance of phosphorus for developing life, whereupon the oxidation of phosphite could have provided energy [73] leading to organophosphates, and ultimately to nucleic acid-based biochemistry.

Methods

Species considered in the batch equilibria models include the gases N_2 , H_2 ; an aqueous solution consisting of H_2O , Ca^{2+} , CaOH^+ , H_2S , HS^- , Fe^{3+} , Fe^{2+} , FeO^+ , FeO_2^- , FeOH^{2+} , FeOH^+ , Fe(OH)_2^+ , Fe(OH)_3^- , Fe(OH)_4^- , H^+ , H_2 , HFeO_2^- , HO_2^- , HPO_3^{2-} , HPO_4^{2-} , H_2PO_2^- , H_2PO_3^- , H_2PO_4^- , HSiO_3^- , $\text{H}_2\text{SiO}_4^{2-}$, H_3SiO_4^- , Cl^- , Mg^{2+} , MgOH^+ , Na^+ , OH^- , PO_4^{3-} , SiO_4^{4-} ; Diopside as $\text{CaMgSi}_2\text{O}_6$; wustite as FeO ; hematite as Fe_2O_3 ; magnetite as Fe_3O_4 ; a brucite solid solution as Fe(OH)_2 , and Mg(OH)_2 ; an olivine solid solution as Fe_2SiO_4 and Mg_2SiO_4 ; a pyroxene solid solution as FeSiO_3 and MgSiO_3 ; a greenalite-serpentine solid solution as $\text{Fe}_3\text{Si}_2\text{O}_5(\text{OH})_4$ and $\text{Mg}_3\text{Si}_2\text{O}_5(\text{OH})_4$; a minnesotaite-talc solid solution as $\text{Fe}_3\text{Si}_4\text{O}_{10}(\text{OH})_2$, and $\text{Mg}_3\text{Si}_4\text{O}_{10}(\text{OH})_2$; a sulfide pH buffer introduced as the salt Na_2S with $\text{H}_2\text{S}(\text{aq})$ in a 1:4 ratio (pH ~ 7.5); quartz as SiO_2 ; phosphorus as solid P_2O_5 and P_2O_3 ; and salt as NaCl .

Laser Raman spectroscopy was utilized to determine the mineral identity. An Enwave μSense Raman microscope operating at 785 nm (Model No. EZI-785-A2) was used. The Raman microscope was a Leica DM300 microscope equipped with three objective lenses ($\times 4/0.1$ NA, $\times 10/0.25$ NA and $\times 40/0.65$ NA).

Integration time is 30 s to 60 s. Crystal Sleuth software was utilized to determine mineral identity. Database searching compared the sample with the RRUFF database [74].

Powder XRD was performed using an Olympus BTX Benchtop XRD (with a Cu cathode) to verify mineral identity further. A calibrated ion chamber, Ludium Model 9 – 3 Radiation Ion Chamber, was obtained for the measurements which measured radiation level counting range of 0 to 2000 $\mu\text{Sv}/\text{Hr}$. Crystal Sleuth software was utilized to determine the mineral identity. Database searching compared the sample with the RRUFF database [74].

Samples of the serpentinite rock were analyzed by X-Ray Fluorescence (XRF) following prior methods [75], at Hamilton College (NY) on a Bruker AXS S8 Tiger Wavelength Dispersive X-Ray Fluorescence (WDXRF).

Serpentinites were collected from southwestern Oregon as part of the Josephine Ophiolite in the Klamath Mountains [69]. Powdered samples were extracted using 15 mL of a 1:4 EDTA NaOH solution, then concentrated, rehydrated with D_2O , and analyzed on a Bruker Neo 600 NMR for 11500 scans in both H-coupled and decoupled modes.

A solution of Na_2HPO_3 (0.05 M) was prepared by reacting NaOH and H_3PO_3 in solution, to which Na_2HPO_4 was added to reach a 0.05 M solution of phosphate, giving a 1:1 phosphite to phosphate mixture consisting of 0.05M of both species. The solution was poured into several vials. To these vials, a solution of 0.1 M CaCl_2 (prepared by mixing anhydrous CaCl_2 in de-ionized water) was added in varying total Ca/P ratios. An 0.8 mL aliquot of the solution within each vial was removed, filtered, and mixed with 0.2 mL of D_2O , and analyzed by ^{31}P NMR, as per Sect. 1.5. 1024 scans were taken for each of these samples.

Declarations

Acknowledgements.

This work was jointly supported by NSF and the NASA Astrobiology Program, under the NSF Center for Chemical Evolution, CHE-1504217, and by the NASA Exobiology program (80NSSCC18K1288).

References

1. D. M. Karl, Microbially mediated transformations of phosphorus in the sea: new views of an old cycle. *Ann. Rev. Marine Sci.* **6**, 279–337 (2014).
2. F. H. Westheimer, Why nature chose phosphates. *Science* **235**, 1173–1178 (1987).
3. G. M. Filippelli, The global phosphorus cycle: past, present, and future. *Elements* **4**, 89–95 (2008).
4. J. K. Lassila, J. G. Zalatan, D. Herschlag, Biological phosphoryl-transfer reactions: understanding mechanism and catalysis. *Ann. Rev. Biochem.* **80**, 669–702 (2011).

5. J. Elser, E. Bennett, E. Phosphorus cycle: a broken biogeochemical cycle. *Nature* **478**, 29–31 (2011).
6. J. E. Goldford, H. Hartman, T. F. Smith, D. Segrè, Remnants of an ancient metabolism without phosphate. *Cell* **168**, 1126–1134 (2017)..
7. F. Wolfe-Simon et al., A bacterium that can grow by using arsenic instead of phosphorus. *Science* **332**, 1163–1166 (2011).
8. M. A. Pasek, J. M. Sampson, Z. Atlas, Redox chemistry in the phosphorus biogeochemical cycle. *Proc. Natl. Acad. Sci. USA* **111**, 15468–15473 (2014).
9. W. Bains, J. J. Petkowski, C. Sousa-Silva, S. Seager, New environmental model for thermodynamic ecology of biological phosphine production. *Sci. Tot. Env.* **658**, 521–536 (2019).
10. M. S. Milman-Barris et al., Zoning of phosphorus in igneous olivine. *Contr. Min. Pet.* **155**, 739–765 (2008).
11. F. Brunet, G. Chazot, Partitioning of phosphorus between olivine, clinopyroxene and silicate glass in a spinel lherzolite xenolith from Yemen. *Chem. Geo.* **176**, 51–72 (2001).
12. E. B. Watson, D. J. Cherniak, M. E. Holycross, Diffusion of phosphorus in olivine and molten basalt. *Am. Min.* **100**, 2053–2065 (2015).
13. S. O. Agrell, N. R. Charnley, G. A. Chinner, Phosphoran olivine from Pine Canyon, Piute Co., Utah. *Min. Mag.* **62**, 265–269 (1998).
14. C-M. Xing, C. Y. Wang, W. Tan. Disequilibrium growth of olivine in mafic magmas revealed by phosphorus zoning patterns of olivine from mafic–ultramafic intrusions. *Earth Planet. Sci. Lett.* **479**, 108–119 (2017).
15. I. Baziotis al., Phosphorus zoning as a recorder of crystal growth kinetics: application to second-generation olivine in mantle xenoliths from the Cima Volcanic Field. *Contr. Min. Pet.* **172**, 58 (2017).
16. J. D. Toner, D. C. Catling, A carbonate-rich lake solution to the phosphate problem of the origin of life. *Proc. Natl. Acad. Sci. USA* **117**, 883–888 (2019).
17. B. Burcar et al., Darwin's warm little pond: a one-pot reaction for prebiotic phosphorylation and the mobilization of phosphate from minerals in a urea-based solvent. *Angew. Chem. Int. Ed.* **55**, 13249–13253 (2016).
18. B. Burcar et al., A stark contrast to modern Earth: phosphate mineral transformation and nucleoside phosphorylation in an iron- and cyanide-rich early Earth scenario. *Angew. Chem. Int. Ed.* **58**, 16981–16987 (2019).
19. N. V. Sobolev et al., Olivine inclusions in Siberian diamonds: high-precision approach to minor elements. *Eur. J. Min.* **20**, 305–315 (2008).
20. J. C. De Hoog, L. Gall, D. H. Cornell, Trace-element geochemistry of mantle olivine and application to mantle petrogenesis and geothermobarometry. *Chem. Geo.* **270**, 196–215 (2010).
21. C. Herzberg, K. Condie, J. Korenaga, Thermal history of the Earth and its petrological expression. *Earth Planet. Sci. Lett.* **292**, 79–88 (2010).

22. E. G. Nisbet, M. J. Cheadle, N. T. Arndt, M. J. Bickle, Constraining the potential temperature of the Archaean mantle: A review of the evidence from komatiites. *Lithos*, **30**, 291–307 (1993).
23. S. A. Wilde, J. W. Valley, W. H. Peck, C. M. Graham, Evidence from detrital zircons for the existence of continental crust and oceans on the Earth 4.4 Gyr ago. *Nature* **409**, 175–178 (2001).
24. C. T. Adcock, E. M. Hausrath, P. M. Forster, Readily available phosphate from minerals in early aqueous environments on Mars. *Nat. Geosci.* **6**, 824–827 (2013).
25. O. L. Kuskov, V. A. Kronrod, Core sizes and internal structure of Earth's and Jupiter's satellites. *Icarus* **151**, 204–227 (2001).
26. O. L. Kuskov, V. A. Kronrod. "Internal structure of Europa and Callisto. *Icarus* **177** 550–569 (2005).
27. C. R. Glein, J. A. Baross, J. H. Waite Jr, The pH of Enceladus' ocean. *Geochim. Cosmochim. Ac.* **162**, 202–219 (2015).
28. M. A. Pasek, D. S. Lauretta, Aqueous corrosion of phosphide minerals from iron meteorites: a highly reactive source of prebiotic phosphorus on the surface of the early Earth. *Astrobiology* **5**, 515–535 (2005).
29. M. A. Pasek, J. P. Dworkin, D. S. Lauretta, A radical pathway for organic phosphorylation during schreibersite corrosion with implications for the origin of life. *Geochim. Cosmochim. Ac.* **71**, 1721–1736 (2007).
30. M. A. Pasek, Rethinking early Earth phosphorus geochemistry. *Proc. Natl. Acad. Sci. USA* **105**, 853–858 (2008).
31. M. A. Pasek, J. P. Harnmeijer, R. Buick, M. Gull, Z. Atlas, Evidence for reactive reduced phosphorus species in the early Archean ocean. *Proc. Natl. Acad. Sci. USA*, **110**, 10089–10094 (2013).
32. M. Gull et al., Nucleoside phosphorylation by the mineral schreibersite. *Sci. Rep.* **5**, 17198 (2015).
33. D. J. Ritson, S. J. Mojzsis, J. D. Sutherland, Supply of phosphate to early Earth by photogeochemistry after meteoritic weathering. *Nat. Geosci.* **13**, 344–348 (2020).
34. B. Herschy et al., Archean phosphorus liberation induced by iron redox geochemistry. *Nat. Comm.* **9**, 1346 (2018).
35. M. A. Pasek, Phosphorus volatility in the early solar nebula. *Icarus* **317**, 59–65 (2019).
36. C. Gibard et al., Geochemical sources and availability of amidophosphates on the early Earth. *Angew. Chem. Int. Ed.* **58**, 8151–8155 (2019).
37. P. J. Cook, M. W. McElhinny. A reevaluation of the spatial and temporal distribution of sedimentary phosphate deposits in the light of plate tectonics. *Econ. Geo.* **74**, 315–330 (1979).
38. S. Porder, S. Ramachandran, The phosphorus concentration of common rocks—a potential driver of ecosystem P status. *Plant Soil* **367**, 41–55 (2013).
39. B. Schink, M. Friedrich, Phosphite oxidation by sulphate reduction. *Nature* **406**, 37–37 (2000).
40. A. K. White, W. W. Metcalf, Microbial metabolism of reduced phosphorus compounds. *Annu. Rev. Microbiol.* **61**, 379–400 (2007).

41. M. Pasek, A role for phosphorus redox in emerging and modern biochemistry. *Curr. Op. Chem. Bio* **49**, 53–58 (2019).
42. T. J. McCoy et al., Formation of vesicles in asteroidal basaltic meteorites. *Earth Planet. Sci. Lett.* **246**, 102–108 (2006).
43. S. L. Brantley, J. D. Kubicki, A. F. White (Eds.), Kinetics of water-rock interaction (Springer, 2008), 833 pp.
44. T. M. McCollom et al., Temperature trends for reaction rates, hydrogen generation, and partitioning of iron during experimental serpentinization of olivine. *Geochim. Cosmochim. Ac.* **181**, 175–200 (2016).
45. H. M. Lamadrid et al., Effect of water activity on rates of serpentinization of olivine. *Nature Comm.* **8**, 1–9 (2017).
46. K. L. Smith, A. R. Milnes, R. A. Eggleton, Weathering of basalt: formation of iddingsite. *Clays Clay Min.* **35**, 418–428 (1987).
47. K. Tomeoka, P. R. Buseck, Matrix mineralogy of the Orgueil CI carbonaceous chondrite. *Geochim. Cosmochim. Ac.* **52**, 1627–1640 (1988).
48. M. Y. Zolotov, E. L. Shock, Energy for biologic sulfate reduction in a hydrothermally formed ocean on Europa. *J. Geophys. Res. Planets* **108**, E001966 (2003).
49. Y. Sekine et al. High-temperature water–rock interactions and hydrothermal environments in the chondrite-like core of Enceladus. *Nat. Comm.* **6**, 1–8 (2015).
50. J. B. Moody, Serpentinization: a review. *Lithos* **9**, 125–138 (1976).
51. M. J. Russell, A. J. Hall, W. Martin, Serpentinization as a source of energy at the origin of life. *Geobio.* **8**, 355–371 (2010).
52. R. E. Hannigan, E. R. Sholkovitz, The development of middle rare earth element enrichments in freshwaters: weathering of phosphate minerals. *Chem. Geo.* **175**, 495–508 (2001).
53. R. Flicoteaux, J. Lucas, “Weathering of phosphate minerals” in Phosphate Minerals J. O. Nriagu, P. B. Moore, Eds. (Springer 1984) pp. 292–317.
54. G. Mallmann, H. St C. O’Neill, S. Klemme. Heterogeneous distribution of phosphorus in olivine from otherwise well-equilibrated spinel peridotite xenoliths and its implications for the mantle geochemistry of lithium. *Contr. Min. Pet.* **158**, 485–504 (2009).
55. C. Oze, M. Sharma, Serpentinization and the inorganic synthesis of H₂ in planetary surfaces. *Icarus* **186**, 557–561 (2007)..
56. F. Klein, W. Bach, T. M. McCollom, Compositional controls on hydrogen generation during serpentinization of ultramafic rocks. *Lithos* **178**, 55–69 (2013).
57. G. Faure, Principles and applications of geochemistry. (Prentice Hall 1997) 600 pp.
58. T. M. McCollom, W. Bach, Thermodynamic constraints on hydrogen generation during serpentinization of ultramafic rocks. *Geochim. Cosmochim. Ac.* **73**, 856–875 (2009).
59. W. Bach et al. Unraveling the sequence of serpentinization reactions: petrography, mineral chemistry, and petrophysics of serpentinites from MAR 15 N (ODP Leg 209, Site 1274). *Geophys. Res. Lett.* **33**,

- L13306 (2006).
60. G. D. Harper, The Josephine ophiolite, northwestern California. *Geo. Soc. Am. Bull.* **95**, 1009–1026 (1984).
 61. Y. Sonzogno, A. H. Treiman, S. P. Schwenzer, Serpentinite with and without brucite: A reaction pathway analysis of a natural serpentinite in the Josephine ophiolite, California. *J. Min. Petrol. Sci.* **112**, 59–76 (2017).
 62. M. A. Pasek et al., Production of potentially prebiotic condensed phosphates by phosphorus redox chemistry. *Angew. Chem. Int. Ed.* **47**, 7918–7920 (2008).
 63. H. J. B. Dick, Terrestrial nickel-iron from the Josephine Peridotite, its geologic occurrence, associations, and origin." *Earth Planet. Sci. Lett.* **24**, 291–298 (1974).
 64. J. A. Bergendahl, T. P. Thies. Fenton's oxidation of MTBE with zero-valent iron. *Water Res.* **38**, 327–334 (2004).
 65. M. J. Russell et al., The drive to life on wet and icy worlds. *Astrobiology* **14**, 308–343 (2014).
 66. A. Gulick, Phosphorus as a factor in the origin of life. *Am. Sci.* **43**, 479–489 (1955).
 67. M. A. Pasek, M. Gull, B. Herschy, Phosphorylation on the early earth. *Chem. Geo.* **475**, 149–170 (2017).
 68. J. Malpas, "Serpentine and the geology of serpentinized rocks" in *The Ecology of Areas with Serpentinized Rocks* (Springer 1992), pp. 7–30.
 69. G. D. Harper, J. B. Saleeby, M. Heizler, Formation and emplacement of the Josephine ophiolite and the Nevadan orogeny in the Klamath Mountains, California-Oregon: U/Pb zircon and $^{40}\text{Ar}/^{39}\text{Ar}$ geochronology. *J. Geophys. Res. Solid Earth* **99**, 4293–4321 (1994).
 70. R. W. McDowell, B. Cade-Menun, I. Stewart, Organic phosphorus speciation and pedogenesis: analysis by solution ^{31}P nuclear magnetic resonance spectroscopy. *Eur. J. Soil Sci.* **58**, 1348–1357 (2007).
 71. P. N. C. Murphy, A. Bell, B. L. Turner, Phosphorus speciation in temperate basaltic grassland soils by solution ^{31}P NMR spectroscopy. *Eur. J. Soil Sci.* **60**, 638–651 (2009).
 72. B. Mysen, Phosphorus speciation changes across the glass transition in highly polymerized alkali silicate glasses and melts. *Am. Min.* **81**, 1531–1534 (1996).
 73. M. A. Pasek Thermodynamics of Prebiotic Phosphorylation. *Chem. Rev.* in press (2020).
 74. T. Laetsch, R. T. Downs, "Software for identification and refinement of cell parameters from powder diffraction data of minerals using the RRUFF Project and American Mineralogist Crystal Structure Databases" in *Abstracts of the 19th General Meeting of the International Mineralogical Association (IMA 2006)*.
 75. T. Feng, C. Lang, M. A. Pasek, The origin of blue coloration in a fulgurite from Marquette, Michigan. *Lithos*, **342**, 288–294 (2019).

Figures

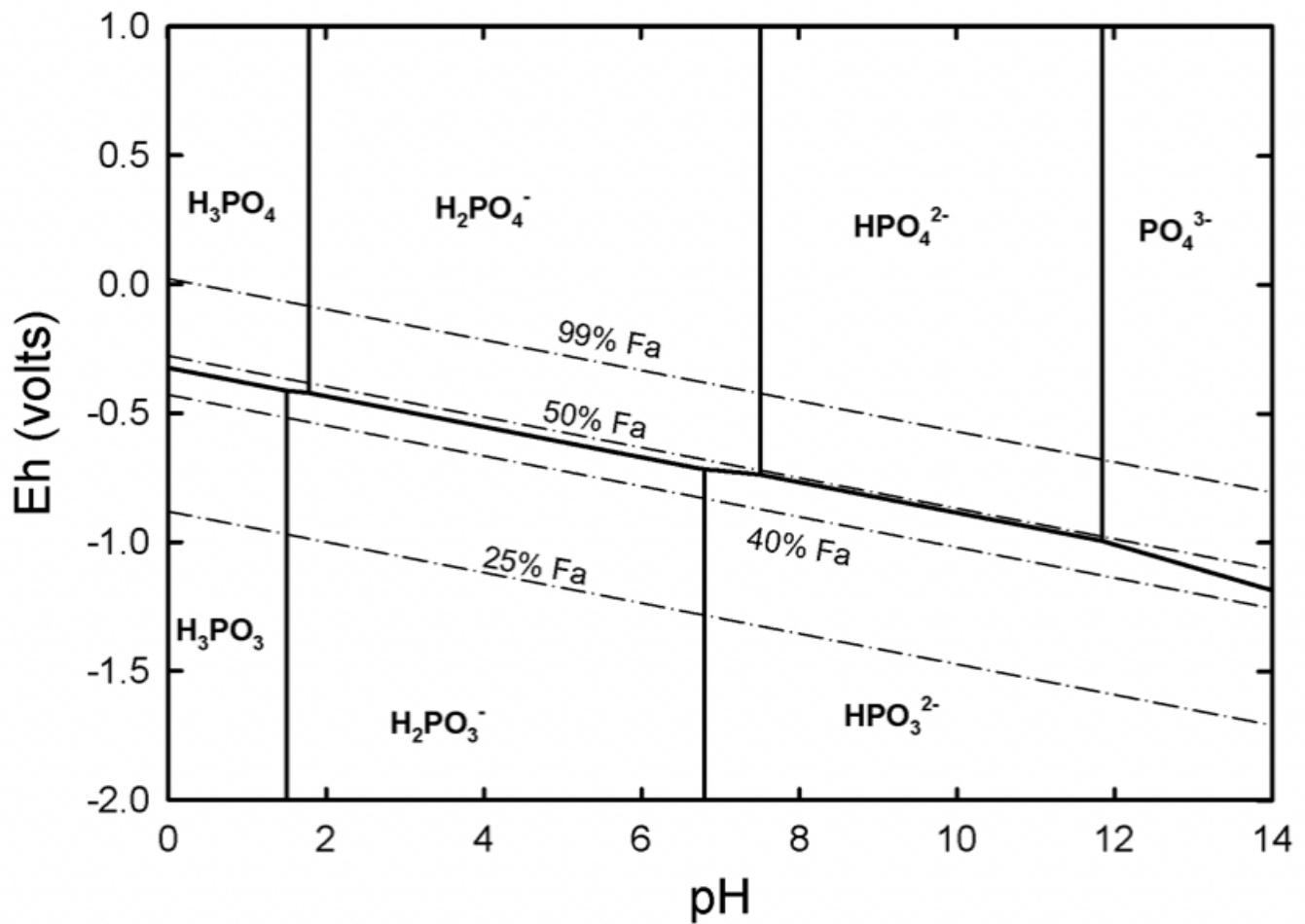


Figure 1

Eh-pH diagram (1 atm, 25°C) for phosphorus (solid lines), with dashed lines showing redox conditions associated with serpentinization of olivine ranging from 99% fayalite to 25% fayalite. Note that solid, non-vertical Eh-pH lines specifically illustrate where the activity of phosphite equals the activity of phosphate (1:1), and that these lines are elevated by about 0.12 V for a 1:100 ratio.

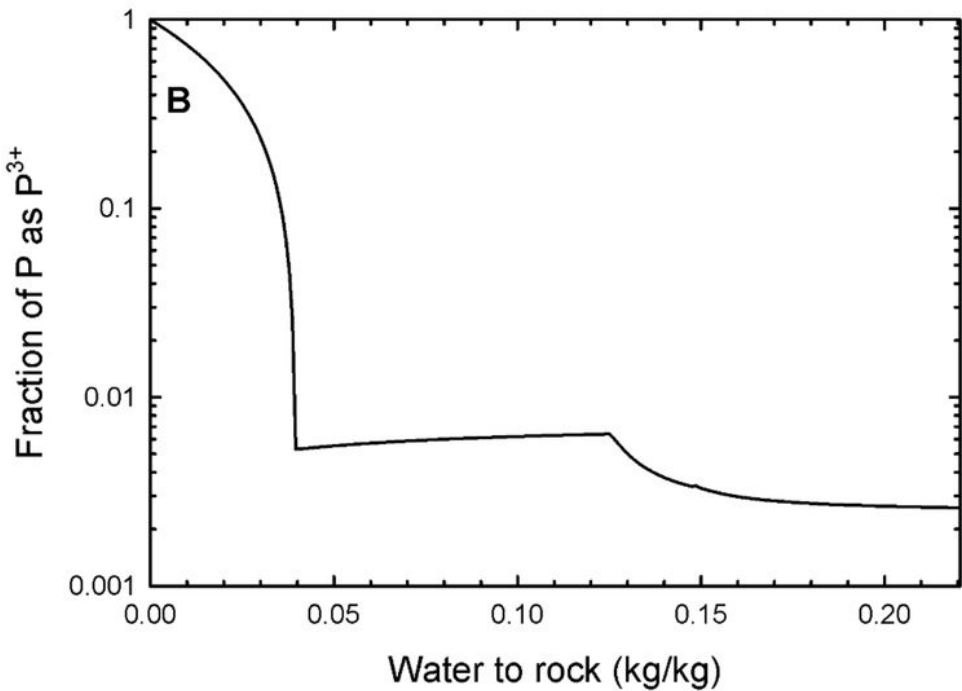
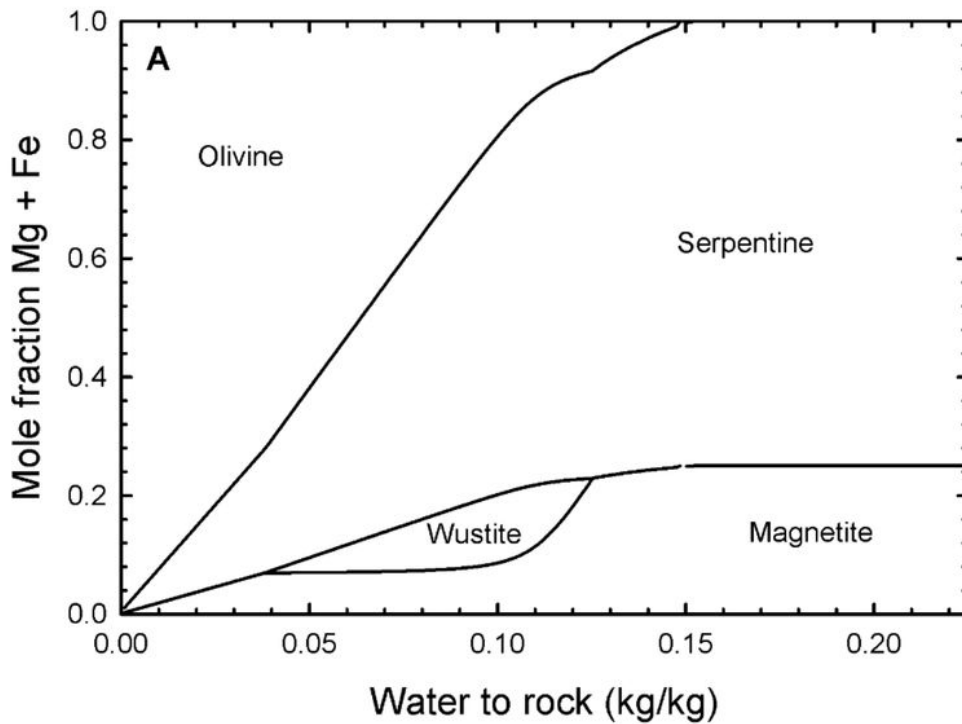


Figure 2

Batch equilibria models of serpentinizing rock, following methods presented by Klein [56]. A) With increasing water content, the olivine hydrates to serpentine with iron oxidizing to wüstite, then to magnetite at these temperatures (in agreement with data from [56], see SI). B) The P speciation is initially almost all reduced at low water-rock ratios, then slowly oxidizes but maintains 0.2-0.3% phosphite as a fraction of all P.

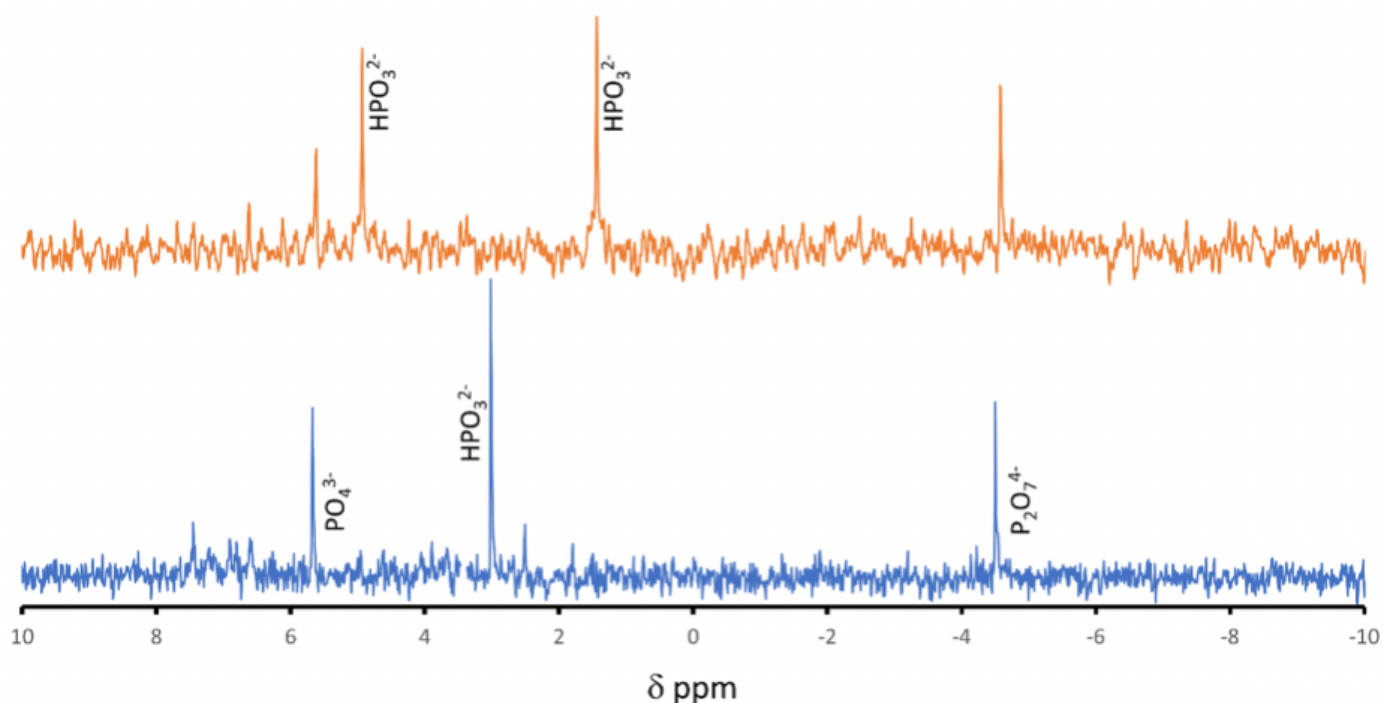


Figure 3

^{31}P NMR spectrum of phosphorus extracted from a serpentinite from Josephine county, OR, USA (pH ~ 13). The x-axis is in ppm, which is a frequency spectrum normalized to 0 for 85% H_3PO_4 . The singlet at 3 ppm (bottom, proton-decoupled) splits into a wide doublet (top, proton-coupled) with a J-coupling constant of 565 Hz and is characteristic of the ion phosphite. The concentration of P measured using this method was about 10^{-4} M with respect to this signal to noise ratio for these scans [29], corresponding to an extraction of about 90% of the total P. The peak at 5.6 ppm is orthophosphate, and at -4.5 ppm is pyrophosphate.

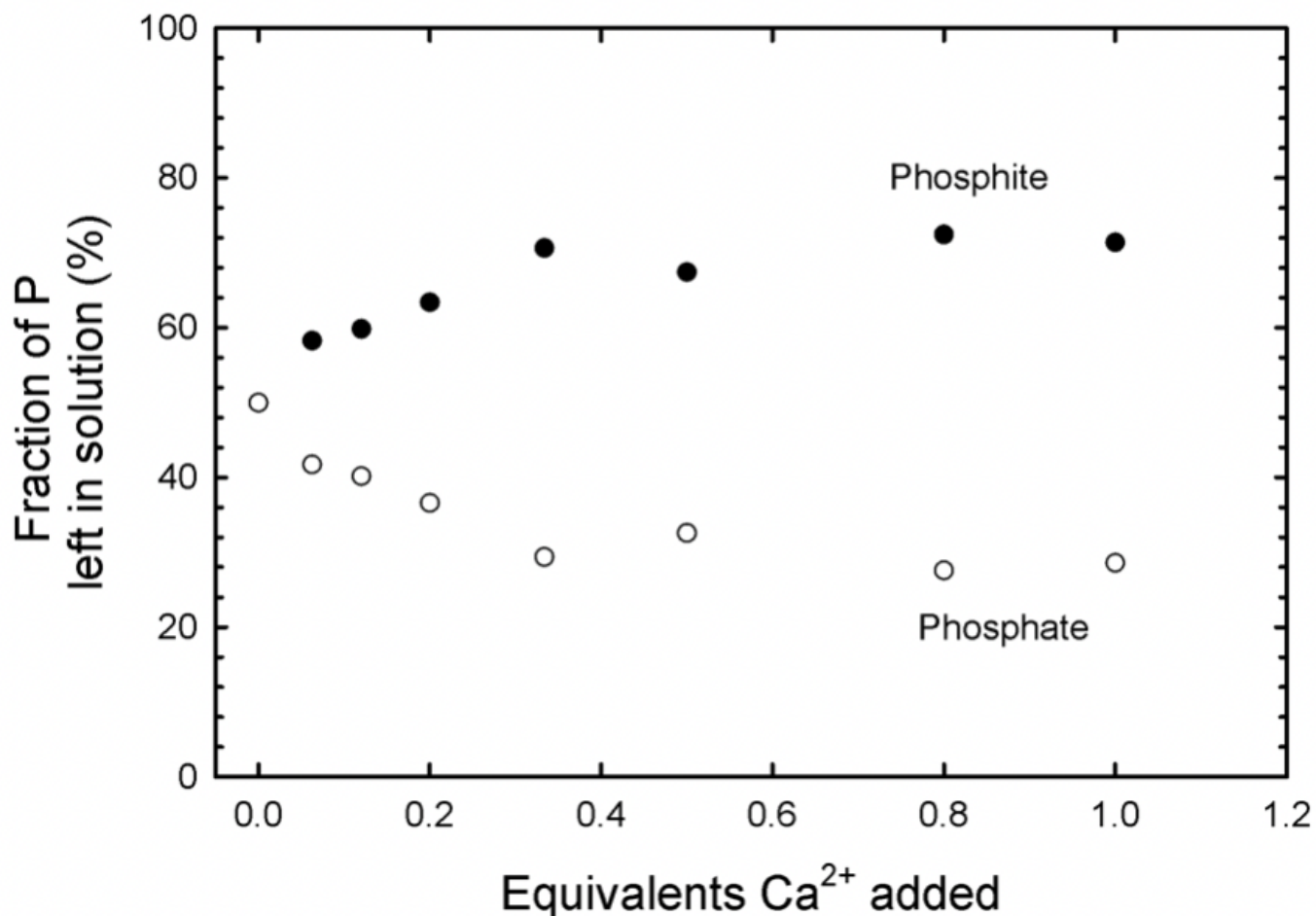


Figure 4

The fraction of initially equimolar (0.05 M) phosphite and phosphate (pH of 8, 25°C) upon the sequential addition of a total of one equivalent (based on Ca/P_{tot}) of CaCl₂ measured by ³¹P NMR. With increasing Ca²⁺, phosphite remains preferentially in solution. Phosphite and phosphate were dissolved as their sodium salts, Na₂HPO₃ and Na₂HPO₄.

Supplementary Files

This is a list of supplementary files associated with this preprint. Click to download.

- [SupplementalInformation.pdf](#)